Application of a figure-of-merit for optical remote sensors to an airborne hyperspectral sensor

E. Tsiang[a], J. Cole[a], M. DeWeert[a], A. Sparks[a], D. Yoon[a], J. Fisher[b], G. Sawai[a], T. Glover[a]
[a]BAE Systems Spectral Solutions LLC, 999 Bishop Street, Honolulu, HI 96813
[b]Brandywine Optics, P. O. Box 459, West Chester, PA 19381

ABSTRACT

Airborne surveillance presents challenging target-detection opportunities for optical remote sensors, especially under the constraints of size, weight, and power imposed by small aircraft. We present a spatial-frequency dependent figure-of-merit, called the Detector Quantum Efficiency (DQE), by first tracing its origins in single pixel photon multiplication detectors, where it is shown to be yield (quantum efficiency or QE) divided by the noise factor. We then show the relationship of DQE to several well-known figures-of-merit. Finally we broaden the definition of DQE to include the spatial-frequency dependence on the MTF of the system and the noise power spectrum (NPS) of the detector. We then present the results of the application of this DQE to a hyperspectral camera under development at BAE Systems Spectral Solutions LLC.

Keywords: Figure-of-merit, detector quantum efficiency, photon transfer curve, Poisson noise, SNR, MTF, noise equivalent quanta, noise equivalent spectral radiance, noise equivalent power, noise figure, D^*, hyperspectral pushbroom sensor, radiometric calibration, Contrast Sensitivity Function, CSF.

1. INTRODUCTION

Automatic target detection, discrimination and identification are the goal of all airborne and spaceborne hyperspectral and multispectral sensors. To satisfy a growing demand in imaging spectrometry, BAE Systems Spectral Solutions LLC has been developing compact hyperspectral sensors (VNIR, SWIR, MWIR) for a variety of flight platforms and cameras (defined as focal plane arrays with supporting electronics). Smaller size, less weight, less operating power with greater performance (spectral range, dynamic range, higher speed, greater resolution) are the key drivers in the new generation of hyperspectral cameras. These systems contain many key submodules: a fore-optics assembly, slit, spectrometer, order-sorting filter and a CCD camera, all of which must contribute to some performance metric or figure-of-merit which represents the radiometric performance and resolving power of the instrument as whole. We introduce such a figure-of-merit in this paper.

Before the spatial context of objects can be recognized, the hyperspectral images must first be reconstructed with the proper spatial character. The key to proper image reconstruction is the characterization of noise and optical imperfections in the system. This characterization or design parameter verification includes photon transfer curves[1], modulation transfer functions (MTF), noise power spectra, noise equivalent power, noise equivalent spectral radiance and other attributes, all of which describe one or other aspect of the electro-optical system. In the end, what is needed is an acceptable common figure-of-merit incorporating all of these methods, valid for a wide variety of image sensors. The need for such a common comparison standard becomes even more pressing with the development of ever more sophisticated sensors[2], both for design and verification. Newer sensors show great promise of suppressing all electronic noise except for inherent Poisson noise, permitting operation in the so-called shot-noise limited regime.

Hyperspectral sensor characterization is divided into three categories: image quality, spectral fidelity (smile and keystone) and radiometric performance[3]. Fortunately, the development of modern sensors has been matched by continuing progress in image quality assessment. A short history of image quality assessment includes: the work of pioneers like Albert Rose[4], the development of concepts like the detective quantum efficiency (DQE) via a branching theory approach by Zweig[5], its generalization to a spatial-frequency dependent DQE by Shaw and his co-workers[6], the transfer matrix information-theoretic approach of Barrett, Cunningham and others[7], and finally, the linkup with signal detectability amidst clutter[8]. One goal of this paper is to explore the consequences of bringing some of these concepts to remote sensing. In particular, we suggest the adoption of Shaw's spatial-frequency dependent DQE, which

brings together measurements of the image quality (MTF), the noise power spectrum (or interpixel correlation of the camera and its supporting amplifier), and the radiometric performance at all spatial frequencies. The fact that this spatial-frequency dependent DQE may have a peak at a certain wave number suggests that the camera is most sensitive to objects of a certain size.

We proceed as follows in this paper:

1. We first show how the single pixel DQE follows from general noise multiplication concepts.
2. We relate this DQE to some well-known figures of merit such as noise equivalent power (NEP), noise equivalent spectral radiance, noise equivalent quanta (Q), and D^*. We exhibit one of the main losses in the hyperspectral system: the grating efficiency.
3. We introduce a generalized spatial-frequency dependent DQE which not only includes the benefits of the figures-of-merit above but also the system MTF and the detector's noise power spectrum (NPS).
4. We evaluate this generalized DQE for a hyperspectral sensor under development at BAE Systems Spectral Solutions LLC.

Our main goal is to provide a framework and establish a nomenclature for the further development and validation of these ideas in the characterization of all hyperspectral and multispectral cameras.

2. STOCHASTIC AMPLIFICATION FOR A SINGLE DETECTOR ELEMENT

In this section we define the noise figure (NF) and detector quantum efficiency (DQE) for a detector operating in a shot noise limited condition, the normal operating regime. In the next section, we introduce noise sources other than shot noise. We begin with space-independent quantities by concentrating on a single detector element or pixel, and then generalize this to space-dependent quantities for a detector array.

The basic detector model is one of stochastic charge multiplication created by an incoming photon. The incoming photon obeys Poisson statistics, and is absorbed in the detector with a probability given by the yield (or quantum efficiency QE_I). We consider this absorption as the $i = 1$ stage of the detection process. Thereafter the secondary electrons may go through a series of multiplication stages $(2 \le i \le N-1)$ which introduce a gain at each stage which has a mean and standard deviation, due to the randomness of charge multiplication (Fig. 1).

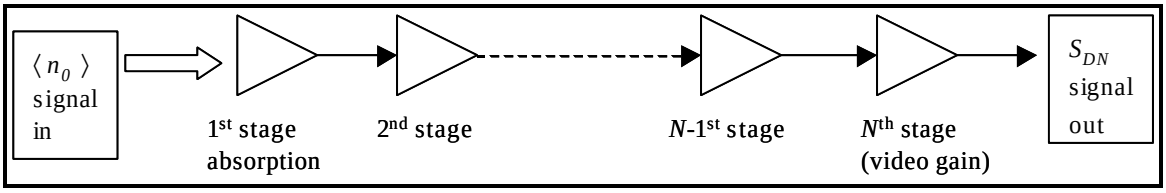

Fig. 1. Photons to photoelectrons to DN units in a charge-multiplying sensor.

The last stage $(i = N)$, which we call "video gain", is typically a conversion from photoelectrons to digital numbers (DN). It is deterministic, and includes A/D circuitry and a scaler.

2.1. Noise figure and detective quantum efficiency

Our approach to charge multiplication is the theory of branching processes, and our starting point is the moment generating function (MGF, or the z-transform of the discrete probability distribution function[9]). At each stage of the multiplication process in a charge-multiplying sensor, each photon (or photo-electron) has the PDF P_n of becoming n photo-electrons. Then the MGF of this PDF is

$$f(z) \equiv \sum_{n=0}^{\infty} P_n z^n \tag{2.1}$$

where z is the complex transform variable. The mean number of daughter photoelectrons and variance are then[10]

$$\langle n\rangle = -\left.\frac{df(z)}{d\ln z}\right|_{z=1} = f'(1) \tag{2.2}$$

$$\langle \Delta n^2\rangle = \langle n^2\rangle - \langle n\rangle^2 = \left.\frac{d^2 \ln f(z)}{(d\ln z)^2}\right|_{z=1} = f''(1) + f'(1) - f'(1)^2 \tag{2.3}$$

respectively, making use of

$$f(1) = 1. \tag{2.4}$$

If we label each stage of the multiplication process by i, where i ranges from 0 (incoming photon, at the zeroth stage) to N, then by the theory of branching processes[11], the overall MGF is given by the iterated function

$$f_{\text{overall}}(z) = f_0\left(f_1\left(f_2\left(\ldots f_N(z)\right)\right)\right) \tag{2.5}$$

with mean and variance definitions given by[12]

$\langle n_0\rangle$, number of incoming photons at the 0^{th} stage, in photon counts or $[\text{ph}]$

$\langle \Delta n_0{}^2\rangle$, variance of incoming photons; $\langle \Delta n_1{}^2\rangle, \ldots, \langle \Delta n_{N-1}{}^2\rangle$, stage variances $\left[\left(\text{pe}^-\right)^2\right]$

$S_{DN} = \langle n_0\rangle R$, signal or final digital number (DN) count, $[\text{DN}]$

$s^2{}_{Shot,DN} = F_{\text{absolute}} R^2 \langle \Delta n_0{}^2\rangle$, variance of final DN count from shot noise, $\left[\text{DN}^2\right]$

$\langle n_1\rangle = QE_l$, 1^{st} stage gain or the quantum efficiency at wavelength l, $\left[\text{pe}^-/\text{ph}\right]$

$\langle n_0\rangle\langle n_1\rangle = \langle n_0\rangle QE_l$, photo-electrons entering the 2^{nd} or beginning of EMG stage, $\left[\text{pe}^-/\text{ph}\right]$ (2.6)

$R \equiv QE_l\ G$, absolute photo-response, $\left[\text{DN}/\text{ph}\right]$

$G \equiv M\ A$, the total system gain, $\left[\text{DN}/\text{pe}^-\right]$

$M \equiv \langle n_2\rangle \ldots \langle n_{N-1}\rangle$, the multiplication gain ratio from amplifier stages 2 to $N-1$

$A \equiv \langle n_N\rangle$, the gain at the final N^{th} stage or video gain, $\left[\text{DN}/\text{pe}^-\right]; \langle \Delta n_N{}^2\rangle = 0$

where we have defined an end-to-end system noise factor called F_{absolute}:

$$F_{\text{absolute}} \equiv \frac{\text{SNR}_{in}{}^2}{\text{SNR}_{out}{}^2} = \frac{\dfrac{s^2{}_{Shot,DN}}{S_{DN}{}^2}}{\dfrac{\langle \Delta n_0{}^2\rangle}{\langle n_0\rangle^2}} = \frac{1}{R^2}\frac{s^2{}_{Shot,DN}}{\langle \Delta n_0{}^2\rangle}$$

$$= 1 + \frac{\langle n_0\rangle}{\langle n_1\rangle^2}\frac{\langle \Delta n_1{}^2\rangle}{\langle \Delta n_0{}^2\rangle} + \frac{\langle n_0\rangle}{\langle n_1\rangle\langle n_2\rangle^2}\frac{\langle \Delta n_2{}^2\rangle}{\langle \Delta n_0{}^2\rangle} + \ldots + \frac{\langle n_0\rangle}{\langle n_1\rangle\langle n_2\rangle\ldots\langle n_{N-1}\rangle\langle n_N\rangle^2}\frac{\langle \Delta n_N{}^2\rangle}{\langle \Delta n_0{}^2\rangle} \tag{2.7}$$

$$= F_1 + \frac{F_2 - 1}{\langle n_1\rangle^2} + \frac{F_3 - 1}{\langle n_1\rangle^2\langle n_2\rangle^2} + \ldots + \frac{F_N - 1}{\langle n_1\rangle^2\langle n_2\rangle^2\ldots\langle n_{N-1}\rangle^2}$$

with noise factors at each stage given by

$$F_i \equiv 1 + \frac{\langle n_0\rangle\langle n_1\rangle\ldots\langle n_{i-1}\rangle\langle \Delta n_i{}^2\rangle}{\langle \Delta n_0{}^2\rangle\langle n_i\rangle^2},\ 1 \le i \le N \tag{2.8}$$

Equation (2.7) for F_{absolute} in terms of the individual noise factors F_i. (2.8)is known as Friis' formula in power amplifier theory[13] and antenna noise temperature theory[14], but in order to be consistent with the stochastic multiplication model, the definition of each F_i differs somewhat from the normal circuit definition of F_i in that the noise $\left\langle \Delta n_i^{\,2} \right\rangle$ at the i^{th} stage is referred back to the source.

2.2. An important special case: noise factor for incoming photons with Poisson and binary absorption statistics

Except for nonideal effects such as dead-time[15] in some high-energy photon counters, the zeroth stage of the stochastic model above is invariably one describing Poisson statistics. In this case,

$$\left\langle \Delta n_0^{\,2} \right\rangle = n_0 \ \left[\text{ph}\right] \tag{2.9}$$

For a simple detector model with no scattering, the next stage is absorption of an incoming photon by the detector material with probability $\left\langle n_1 \right\rangle = QE_l$ and a variance of $\left\langle \Delta n_1^{\,2} \right\rangle = QE_l \left(1 - QE_l\right)$ in a PDF with only two choices: absorption or transmission. With these values, the noise factor becomes

$$F_{\text{absolute}} = \frac{F}{QE_l} \tag{2.10}$$

where the part of F_{absolute} independent of QE_l, designated F, is attributed to the amplifier alone:

$$F \equiv 1 + \frac{\left\langle \Delta n_2^{\,2} \right\rangle}{\left\langle n_2 \right\rangle} + \ldots + \frac{\left\langle \Delta n_N^{\,2} \right\rangle}{\left\langle n_2 \right\rangle \ldots \left\langle n_{N-1} \right\rangle \left\langle n_N \right\rangle} = 1 + \frac{1+\text{PE}_2}{\left\langle n_2 \right\rangle} + \ldots + \frac{1+\text{PE}_N}{\left\langle n_2 \right\rangle \ldots \left\langle n_{N-1} \right\rangle \left\langle n_N \right\rangle} \tag{2.11}$$

with the Poisson excess (equal to zero at the i^{th} stage if that stage obeys strict Poisson statistics) defined as

$$\text{PE}_i \equiv \frac{\left\langle \Delta n_i^{\,2} \right\rangle - \left\langle n_i \right\rangle}{\left\langle n_i \right\rangle} \tag{2.12}$$

If stochastic multiplication noise were the only source of noise, we may define detector quantum efficiency as the inverse of the overall noise factor:

$$\text{DQE} \equiv \frac{1}{F_{\text{absolute}}} = \frac{QE_l}{F} = \frac{\text{SNR}_{\text{out}}^{\,2}}{\text{SNR}_{\text{in}}^{\,2}} = \frac{R^2 \left\langle \Delta n_0^{\,2} \right\rangle}{s^{\,2}_{Shot,DN}} = \frac{\left\langle n_0 \right\rangle R^2}{s^{\,2}_{Shot,DN}} \tag{2.13}$$

The DQE is therefore essentially the QE reduced by the noise factor. If the multiplication gains were deterministic (no gain variances), the DQE would be equal to the QE.

2.3. Shaw's noise equivalent quanta (NEQ) and Janesick's photon transfer curve (PTC) for shot-noise limited detectors

The output squared SNR is given a special definition, the noise equivalent quanta (NEQ)[16]

$$\text{SNR}_{\text{out}}^{\,2} = \frac{S_{DN}^{\,2}}{s^{\,2}_{Shot,DN}} = \text{DQE} \times \text{SNR}_{\text{in}}^{\,2} = \left\langle n_0 \right\rangle \text{DQE} = \left\langle n_0 \right\rangle \frac{QE_l}{F} \equiv \text{NEQ} \tag{2.14}$$

Therefore,

$$s^{\,2}_{Shot,DN} = \frac{RS_{DN}}{\text{DQE}} = FGS_{DN} \ \left[\text{DN}^2\right] \tag{2.15}$$

A graph of $s^{\,2}_{Shot,DN}$ vs. S_{DN} has a slope of a modified overall gain $F_{\text{absolute}} R = FG$. This is in fact Janesick's photon transfer curve (PTC) without the constant background noise term. The PTC provides a way to extract the total system gain G if F were known, at least in principal.

2.4. Experimental results for photo-response factor, noise factor, photon transfer curves, and yield

The linearity of a charge-multiplying sensor can be checked. Fig. 2 gives the plot of signal S_{DN} vs. $\left\langle n_0 \right\rangle$ with slope $R = QE_l G$.

Experimental values for F as a function of gain ratio G has been obtained by DeWeert et al. [17] for a charge-multiplying sensor. Using narrow-band light, they followed Robbins and Hadwen in plotting the PTC of $\frac{s^2_{Shot,DN}}{G}$ against S_{DN}, which has a slope F above the fixed read noise floor (Fig. 3).

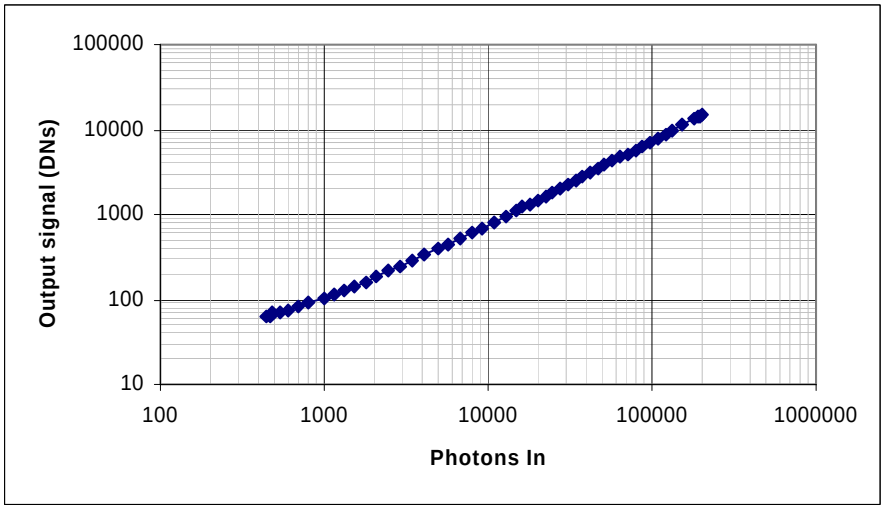

Fig. 2. Output signal S_{DN} vs. input photons $\langle n_0 \rangle$ with slope R in the photon limited region.

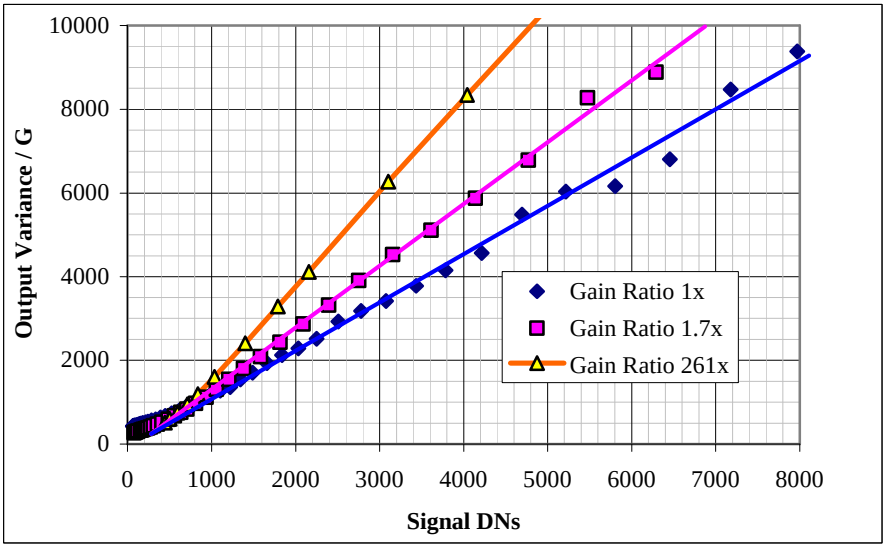

Fig. 3. $s^2_{Shot,DN}/G$ vs. S_{DN}. The slope is *F* for the portion well above the noise floor.

They then obtained the noise figure *F* as a function of *G* in Fig. 4.

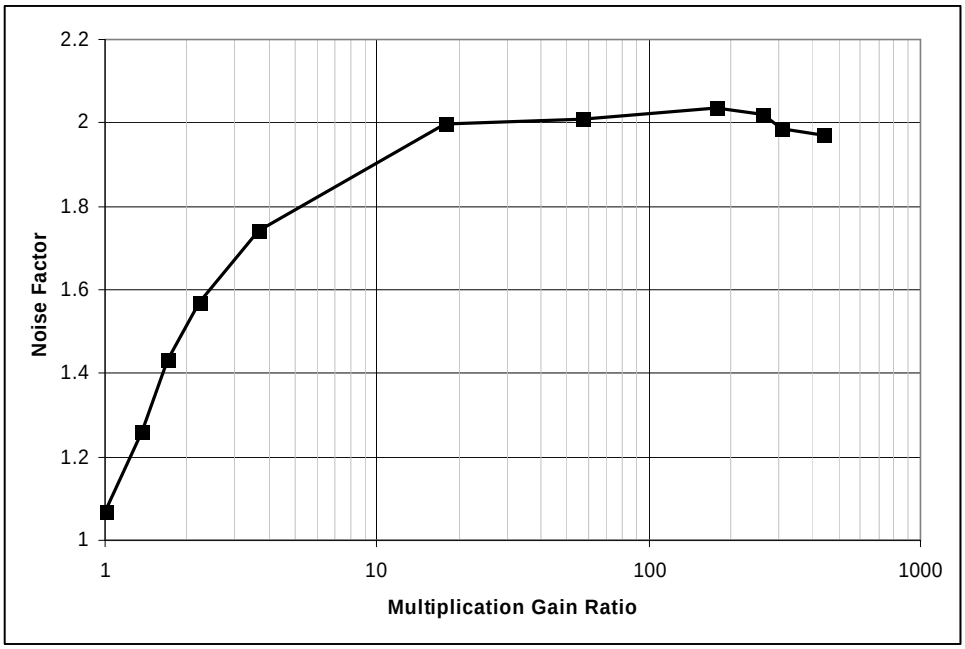

Fig. 4. Noise factor F vs. gain ratio G .

This is in line with the type of behavior for F derived by Bell[19] and McIntyre[20] for multiplication devices like microchannel plates and avalanche photodiodes incorporating both electron and hole multiplication. The exact physical model for any particular charge-multiplying sensor requires a thorough understanding of the underlying photonics.

2.5. Connection of DQE with NESR, NEP and D^*

A number of commonly used benchmarks make use of light power, instead of quanta. In this picture, the incoming photon number is

$$\langle n_0 \rangle = \frac{t(n)\, I_n(\hat{n})\, \Delta n\, \Delta\Omega\, \Delta A}{hn} 2T = \frac{\text{NEQ}}{\text{DQE}} \quad [\text{ph}] \tag{2.16}$$

where

$\Delta\Omega\Delta A =$ throughput etendue $\left[Sr\ cm^2\right]$

$T =$ measurement time $= \dfrac{1}{2B}$ $[s]$

$B =$ noise bandwidth $[Hz]$

$n =$ center frequency of light $[Hz]$ (2.17)

$\Delta n =$ frequency band (light) $[Hz]$

$h =$ Planck's constant $[J\ s]$

$I_n(\hat{n}) =$ specific intensity or brightness for a given direction $\hat{n}$ $\left[WHz^{-1}Sr^{-1}cm^{-2}\right]$

$t(n) =$ transmission loss from source up to sensor

The noise equivalent spectral radiance (NESR) is the brightness which gives a particular output NEQ[21], viz.

$$\text{NESR} \equiv I_n(\hat{n})\big|_{\text{NEQ}} = \frac{\text{NEQ}\ \sqrt{B}\ hn}{t(n)\sqrt{2T}\ \Delta n\ \Delta\Omega\ \Delta A\ \text{DQE}} = \frac{\text{NEQ}}{\sqrt{2T}\ D^*\ t(n)\ \Delta n}\left(\frac{4F^{\#2}}{p\sqrt{\Delta A}}\right) \left[WSr^{-1}cm^{-2}Hz^{-1}\right] \tag{2.18}$$

where $F^{\#} \equiv \dfrac{\text{focal length}}{\text{lens diameter}}$, and we have used some industry-wide figure-of-merits: D^* and noise-equivalent power NEP:

$$D^* = \frac{\sqrt{\Delta A}\sqrt{B}}{B h n}\text{DQE} = \frac{\sqrt{\Delta A}\sqrt{B}}{\text{NEP}} \left[cm\ Hz^{\frac{1}{2}} W^{-1} \right]$$
$$\text{NEP} = B\text{NEP}^* \left[W \right], \text{ and } \quad \text{NEP}^* = \frac{h n}{\text{DQE}} \left[J \right] \tag{2.19}$$

Thus except for a proportionality constant, D^* is essentially the DQE.

2.6. NESR AND NEQ FOR PUSHBROOM SENSORS

To avoid smearing in pushbroom sensors, the integration time cannot be greater than the time it takes to cover the ground sample distance (GSD) for a platform moving with ground speed v_g. With

$$T = \frac{GSD}{v_g} \left[s \right]$$
$$f = \text{focal length} = \frac{H}{GSD}\sqrt{\Delta A} \left[mm \right] \tag{2.20}$$
$$A_c = \text{ clear aperture area } \left[mm^2 \right]$$

we get

$$\text{NESR} = \frac{\text{NEQ}\, fH\sqrt{v_g}}{\sqrt{2} D^* t\left(n\right) \Delta n\, A_c} \left(\frac{1}{GSD^{\frac{3}{2}}} \right) \left[WSr^{-1} cm^{-2} Hz^{-1} \right] \tag{2.21}$$

where A_c is the area of clear aperture. Conversely, a broadband source with specific intensity I_n, the broadband NEQ can be calculated from the formula

$$\text{NEQ}_{\text{broadband}} = \sqrt{\frac{2}{v_g}} \frac{A_c}{fH} GSD^{\frac{3}{2}} \int_{n_1}^{n_2} t\left(n\right) D^* I_n \, dn \tag{2.22}$$

The transmission loss factor $t\left(n\right)$ includes variables which depend on the environment, such as atmospheric losses, ground albedo, geometrical factors[22], and fore-optics losses of the system. But for spectrometers, one of the biggest wavelength-dependent losses is the intrinsic grating efficiency. Grating efficiency is highest for blazed gratings produced by high-cost lithographic methods. "Holographic" gratings produced by interference methods may be used instead for prototyping because of their relatively low cost. BAE Systems have used both types in their sensors. Typical normalized grating efficiencies, calculated using the Kirchhoff approximation[23], are shown in Fig. 5.

3. DQE AND NOISE FIGURE WITH GENERAL NOISE TERMS

We can generalize the quantities we defined previously to the case where additional noise terms other than Poisson noise become important. We find that the only term that needs modification is the overall noise figure, which becomes:

$$F_{\text{overall}} = \left(1 + \frac{P_{\text{dark multiplied}}}{P_n} \right) F + \frac{P_{\text{dark surface unmultiplied}}}{G^2 P_n} + \frac{P_{\text{bias}}}{G^2 P_n B} \tag{3.1}$$

where

$P_{\text{dark multiplied}}$ = bulk dark power, multiplied at each stage of amplifier
$P_{\text{surface unmultiplied}}$ = surface dark power, unmultiplied at each stage of amplifier
P_{read} = mean square read noise
$P_n = I_n\left(\hat{n}\right) \Delta n\ \Delta\Omega\ \Delta A =$ incident power
(3.2)

It is possible to include additional noise terms depending on the particular detector, but this expression agrees with the one derived by Bell. When the noise equivalent power is substituted for P_n, we get

$$\mathrm{DQE} = \frac{QE_l}{F\left(1+\dfrac{\sqrt{P_{\mathrm{read}}m^2 + B\left(G_{\mathrm{overall}}{}^2\left(P_{\mathrm{dark\ multiplied}}Fm^2 + BF^2\ \mathrm{NEQ}\right)\right) + m^2P_{\mathrm{surface}}}}{BF\sqrt{\mathrm{NEQ}}}\right)} \tag{3.3}$$

and this is the expression for DQE to be used in D^* for this general case. Note that the dependence on NEQ goes away for shot-noise limited operation.

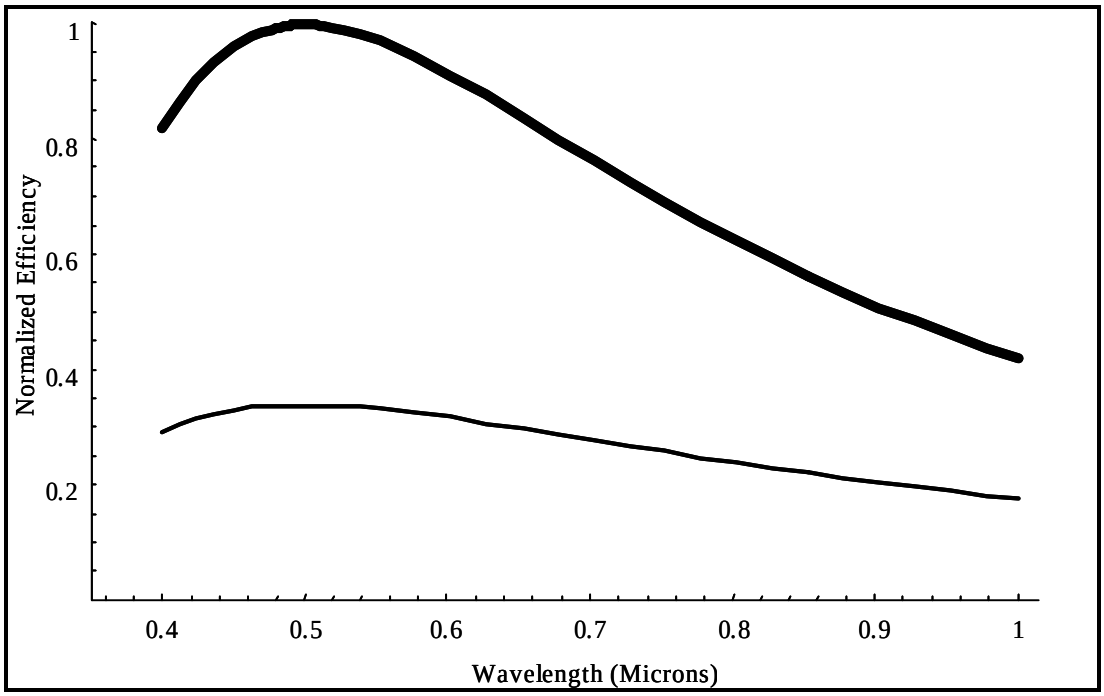

Fig. 5. Normalized theoretical grating efficiency as a function of wavelength, for blazed (upper) and holographic gratings (lower).

4. GENERALIZED DQE AS A FIGURE OF MERIT: STOCHASTIC AMPLIFICATION FOR DETECTOR ARRAYS

For a single pixel, we have related the known figure-of-merits to the DQE. We now generalize this DQE to include linear array and area detectors. First we notice that the incident power P_n contains the useful portion of the signal P_{target} as well as the clutter P_{clutter}. The difference between the two may be defined as a contrast:

$$m^2 = \left(\frac{P_{\mathrm{target}} - P_{\mathrm{clutter}}}{P_{\mathrm{target}} + P_{\mathrm{clutter}}}\right)^2 \tag{4.1}$$

As this contrast has no spatial wavelength dependence, it seems natural to generalize DQE to DQE $m^2\mathrm{MTF}^2$. This has indeed been put on a logical statistical basis by Shaw[24], Rabbiani, Mulder,[25] and others, who absorbed the MTF into the definition of a spatial-frequency dependent $\mathrm{DQE}(\mathbf{k})$, as follows:

$$\underbrace{\mathrm{DQE} = \frac{\langle n_0 \rangle R^2}{s^2_{Shot,DN}}}_{\text{single pixel}} \quad \longrightarrow \quad \underbrace{\mathrm{DQE}(\mathbf{k}) = \frac{R^2 n_o}{\mathrm{NPS_d}(\mathbf{k})} \underbrace{m^2}_{\substack{\text{contrast} \\ \text{factor}}} \mathrm{MTF}^2(\mathbf{k})}_{\text{detector array}} \tag{4.2}$$

where $\mathbf{k}$ is the spatial frequency, and the output noise power spectrum $\mathrm{NPS_d}(\mathbf{k})$ and MTF have the respective normalizations $\int_{-\infty}^{\infty} \mathrm{NPS_d}(\mathbf{k}) d\mathbf{k} = s^2_{Shot,DN}$ and $\mathrm{MTF}(0) = 1$ The noise power spectrum is defined as[26]

$$\mathrm{NPS}_d(\mathbf{k}) \equiv \lim_{\mathbf{X}\to\infty} \left\langle \left| F_{\mathbf{X}}(\Delta d(\mathbf{x})) \right|^2 \right\rangle \tag{4.3}$$

where $F_{\mathbf{X}}(\ )$ is the Fourier transform in the region of interest $\mathbf{X}$, and $\Delta d(\mathbf{x})$ is the zero-mean random scene, with suitable modifications for discrete Fourier transforms. It is equal to the Fourier transform of the autocovariance function.

Once $\mathrm{DQE}(\mathbf{k})$ has been defined, all other spatial-frequency figures-of-merit such as $D^*(\mathbf{k})$ and $\mathrm{NEP}(\mathbf{k})$ can be defined in terms of it, as we did above for a single pixel detector. All the formulae derived in the earlier sections can be rewritten with this spatial-frequency dependence the only modification. Cunningham and Shaw[27] have reviewed the history of $\mathrm{DQE}(\mathbf{k})$ and its accompanying signal- and noise-transfer theory. The modeling of $\mathrm{DQE}(\mathbf{k})$ of staged detector systems in increasing detail, incorporating stochastic amplification and scattering both in series and parallel[28], and noise aliasing due to varying modes of image transfer[29], in the context of Poisson point processes, is an ongoing branch of research. $\mathrm{DQE}(\mathbf{k})$ was initially introduced to describe the noise-limited detectability of low-contrast structures in a uniform background; so its information-theoretic justification[30], for Gaussian and Poisson noise, and its relationship to iterative image reconstruction methods, awaits further study.

4.1. MTF, DQE and NPS results

The MTF of a typical detector used in a multispectral or hyperspectral sensor is shown in Fig. 6[31].

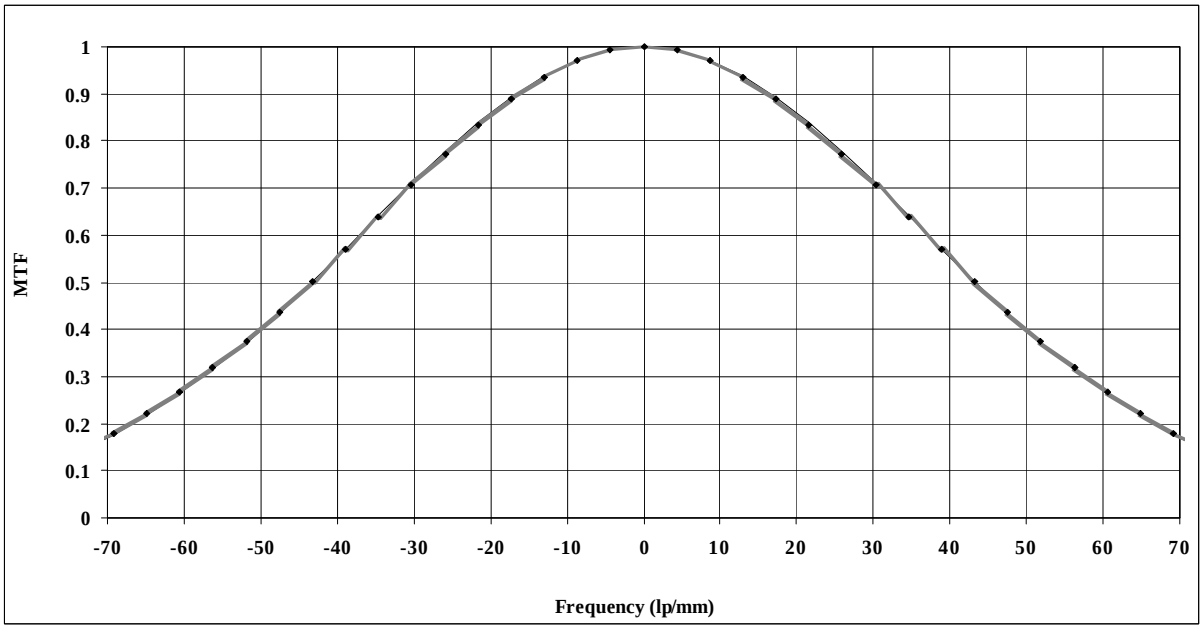

Fig. 6. Sensor MTF for a multispectral or hyperspectral sensor up to the Nyquist limit.

For both multispectral and hyperspectral cameras, one of the camera axes is chosen to be parallel to the motion (along-track direction) and the other transverse to the motion, but for hyperspectral cameras in a pushbroom configuration, the along-track direction is also the direction of spectral dispersion. In this spectral direction, there is a direct translation of length (mm) into photon wavelength (nm), leading to a relabeling of the abscissa units in Fig. 6 from lp/mm to lp/nm). At the same time, the finite width of the slit, which masks off the entire scene except for a width equivalent to one IFOV, admits some spatial components into the spectral direction as well. We will discuss the implications of these subtleties in a future study. For the moment we can assume that the concept of MTF applies equally well without modification to both multispectral and hyperspectral sensors.

The normalized noise power spectrum, defined as $\mathrm{NPS_d}(\mathbf{k})/s^2_{Shot,DN}$ for the same camera is shown in Fig. 7:

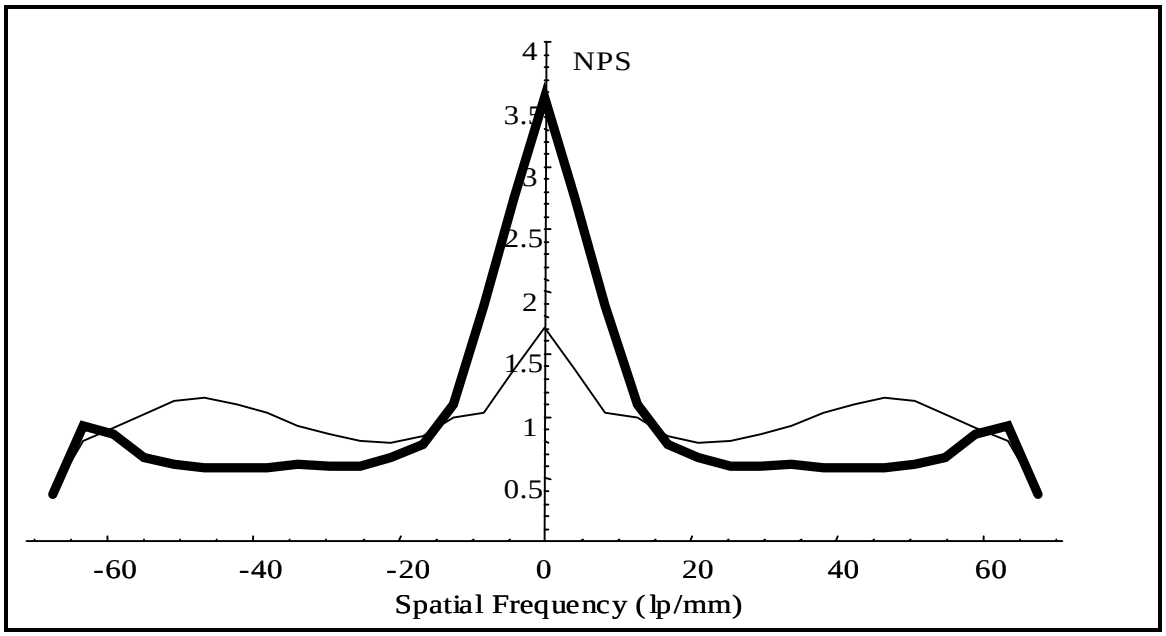

Fig. 7. Normalized noise power spectrum for CCD camera in pushbroom configuration as a function of spatial frequency. Thick line – spatial direction cross-track, thin line – spectral direction, along-track.

The small peak at higher frequencies may be an indication of the presence of periodic fixed pattern noise both in the along-track and cross-track directions. The difference in the response in the two directions may have several causes, such as an intrinsic difference in cross-pixel correlations along different directions, or differences in how the image is read out in the different directions.

The ratio

$$\frac{\mathrm{DQE}(\mathbf{k})\ s^2_{Shot,DN}}{\langle n_0 \rangle R^2} = \mathrm{DQE}(\mathbf{k})\ F_{\mathrm{absolute}} = \frac{\mathrm{DQE}(\mathbf{k})\ F}{QE_l} = \frac{\mathrm{MTF}^2(\mathbf{k})}{\left[\dfrac{\mathrm{NPS_d}(\mathbf{k})}{s^2_{Shot,DN}}\right]} \tag{4.4}$$

has a peak at a wavenumber which is not zero (Fig. 8). The existence of an optimal spatial frequency for contrast sensitivity is well known from studies of the contrast sensitivity function (CSF) of the human visual system[32,33], which peaks at about 4 cycles/degree. The differences in the DQE in the two directions, the implications of peaks in the DQE, and the relationship of DQE to the CSF, await further study.

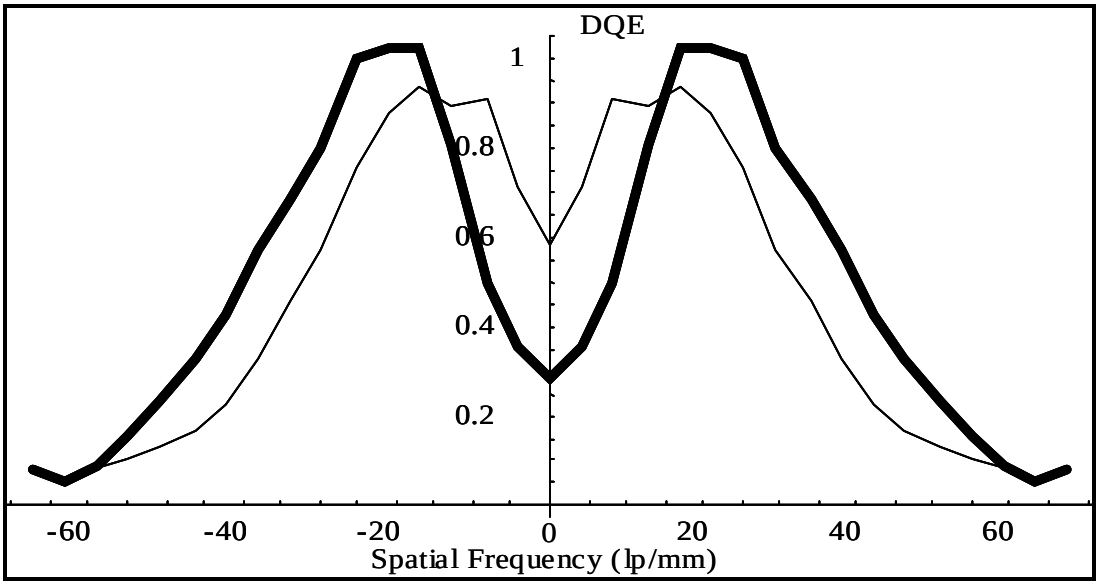

Fig. 8.Normalized DQE for CCD camera in pushbroom configuration as a function of spatial frequency. Thick line – spatial direction cross-track, thin line – spectral direction, along-track.

5. CONCLUSIONS

We have proposed a figure-of-merit called the DQE which underlies the definition of almost all radiometric figures-of-merit such as NEQ and D^* can. We showed how this DQE is just the yield (quantum efficiency) divided by the noise figure for a single pixel. We also demonstrated how almost all conventional figures of merit can be expressed in terms of it. We then generalized this DQE to camera arrays with vector wavenumber dependence. For hyperspectral sensors, the wavenumber along-track is the spectral dimension, and the wavenumber cross-track is the spatial dimension. We presented an example of a typical spatial-frequency dependent DQE calculation for a hyperspectral camera, and showed how the instrument is most sensitive to features of a certain size. This leads to the interesting question of how this will relate to observer dependent measures such as receiver operating characteristics. The exact connection with this and other detectability metrics, and the validation of these metrics, will be the subject of future investigations.

6. ACKNOWLEDGEMENTS

The authors thank Dr. Doug Todoroff (Office of Naval Research) and Mr. Ned Witherspoon (Naval Surface Warfare Center) for their review and comments on this manuscript.

REFERENCES

1 J. R. Janesick, Scientific Charge-Coupled Devices, SPIE Press, Bellingham, WA 2001.

[2]M. S. Robbins and B. J. Hadwen, "The noise performance of electron multiplying charge coupled devices", IEEE Transactions on Electron Devices, 2003, 50, 1227-1232

[3] C. O. Davis, J. Bowles, R. A. Leathers, D. Korwan, T. V. Downes, W., A. Snyder, W. J. Rhea, W Chen, J. Fisher, W. P. Bissett and R. A. Reisse, "Ocean PHILLS hyuperspectral imager: design, characterization, and calibration", Optics Express 10, #4, 2002.

[4] A. Rose, "Sensitivity performance of the human eye on an absolute scale", Journal of the Optical Society of America, 38, 196-208, 1948.

[5] H. J. Zweig, "Detective quantum efficiency of photodetectors with some amplifying mechanism", Journal of the Optical Society of America 55, pp 525-528, 1965.

[6] M. Rabbani, R. Shaw and R. Van Metter, "Detector quantum efficiency of imaging systems with amplifying and scattering mechanisms", Journal of the Optical Society of America A, Vol. 4, No. 5, pp. 895-901, 1987.

[7] J. Yao and I. A. Cunningham, "Parallel cascades: new ways to describe noise transfer in medical imaging systems", *Medical Physics*, 28(10), pp 2020 – 2038, 2001.
[8] H. H. Barrett and K. Myers, *Foundations of Image Science*, Wiley Interscience, NY, 2003.
[9] L. R. Rabiner and B. Gold, *Theory and Application of Digital Signal Processing*, Prentice-Hall, NJ, 1973.
[10] B. Saleh, *Photoelectron Statistics*, Springer-Verlag, Berlin, 1978.
[11] T. E. Harris, *The Theory of Branching Processes*, Dover reprint, Mineola, NY, 1989.
[12] All units pertaining to the quantities are enclosed within [ ].
[13] G. Gonzalez, *Microwave Transistor Amplifiers*, 2nd edition, Prentice-Hall, NJ, 1996.
[14] K. Rohlfs and T. L. Wilson, *Tools of Radio Astronomy*, 4th edition, Springer-Verlag, Berlin, 2003.
[15] G. F. Knoll, *Radiation Detection and Measurement*, 2nd edition, Wiley, NY , 1989.
[16] J.C. Dainty and R. Shaw, *Image Science*, Academic Press, NY, 1974.
[17] M. J. DeWeert, J. B. Cole, A. W. Sparks and A. Acker, "Photon transfer methods and results using EMCCDs", *SPIE 49th Annual Meeting*, this conference, 2004.
[19] R. L. Bell, "Noise figure of the MCP image intensifier tube", *IEEE Transactions of Electron Devices*, ED-22, 10, pp 821-829, 1975.
[20] P. P. Webb, R. J. McIntyre and J. Conradi, "Properties of avalanche photodiodes", *RCA Review*, 35, pp 234-278, 1974.
[21] Sometimes NESR is defined so that it refers to the power in a specific wavelength band. The unit is then $\left[WSr^{-1}cm^{-2}nm^{-1}\right]$, defined as a microflick.
[22] M. Born and E. Wolf, *Principles of Optics*, 5th edition, Pergamon Press, Oxford, 1975.
[23] P. Beckmann and A. Spizzichino, *The Scattering of Electromagnetic Waves from Rough Surfaces*, Artech House, Norwood, MA, 1987.
[24] R. Shaw, "The equivalent quantum efficiency of the photographic process" *J. Photogr. Sc.* 11, pp 199-204, 1963.
[25] H. Mulder, "Signal and noise transfer through imaging systems consisting of a cascade of amplifying and scattering processes", *Journal of the Optical Society of America A*, 10, pp 2038 – 2045, 1993.
[26] H. Lai and I. A. Cunningham, "Noise aliasing in interline-video-based fluoroscopy systems", *Med. Phys*. 29(3), pp. 298-310, 2002.
[27] I. A. Cunningham and R. Shaw, "Signal-to-noise optimization of medical imaging systems", *Journal of the Optical Society of America* A, 16, pp 621-632, 1999.
[28] J. Yao and I. A. Cunningham, "Parallel cascades: new ways to describe noise transfer in medical imaging systems", *Med. Phys.* 29 (10), pp 2029 – 2038, 2001.
[29] I. A. Cunningham, J. Yao and V. Subotic, "Cascaded models and the DQE of flat-panel imagers: noise aliasing, secondary quantum noise and reabsorption", *Med. Imaging 2002: Physics of Medical Imaging, Proc. SPIE* 4682: 61-72, 2002.
[30] F. O. Huck, C. L. Fales and Zia-ur Rahman, *Visual Communications: an Information Theory Approach*, Kluwer Academic, Boston, 1997.
[31] Data provided by A. W. Sparks, M. J. DeWeert, C. L. Stalder, J. B. Cole, BAE Systems Spectral Solutions, LLC.
[32] F. Campbell and J. Robson, "Application of Fourier analysis to the visibility of gratings" *Journal of Physiology*, 197:551–566, 1968.
[33] Marcus Nadenau, "Integration of Human Color Vision Models into High Quality Image Compression," *École Polytechnique Fédérale De Lausanne, Thesis No 2296*, Lausanne, Switzerland, 2000.